

# MBTree: Detecting Encryption RAT Communication Using Malicious Behavior Tree

Cong Dong<sup>1,2</sup>, Zhigang Lu<sup>1,2</sup>, Yufan Chen<sup>3</sup>, Zelin Cui<sup>1,2</sup>, and Baoxu Liu<sup>1,2</sup>

<sup>1</sup>*Institute of Information Engineering, Chinese Academy of Sciences*

<sup>2</sup>*School of Cyber Security, University of Chinese Academy of Sciences*

<sup>3</sup>*Information Police Institute, China Industrial Control Systems Cyber Emergency Response Team*

## Abstract

A key challenge for cybersecurity defense is to detect the encryption Remote Control Trojan (RAT) communication traces. It is still an open research problem to detect encryption RAT precisely in different environments. Previous studies in this area either cannot handle the encrypted content or perform unstable in a different environment. To tackle both problems, we present MBTree, a novel host-level signature based approach for encryption RAT traffic detection. MBTree consists of a structure named MLTree and a similarity matching mechanism. The MLTree integrates multiple directed packet payload size sequences as a host signature. Furthermore, the matching mechanism compares two MLTree to decide if an alarm is triggered. Compared with previous related studies, MBTree (i) is more accurate to characterize different encryption RATs; (ii) has more robust performance when emerging new benign applications in the test environment; (iii) can automatically create signatures from malicious traffic without requiring human interaction. For evaluation, we collect traffic from multiple sources and reorganize them in a sophisticated manner. The experiment results demonstrate that our proposed method is more precise and robust, especially in the situation with new emerging applications.

## 1 Introduction

Modern network attacks are accomplished with advanced automatic tools. One of them used in the post-penetration procedure is the *RAT with encrypted tunnels*. These types of RAT can lurk in the victim machine for a long time to complete damage operation and steal confidential files [5]. While specifying RAT activities can cut off the kill chain and prevent further losses. It is of great importance for RAT detection.

The traditional RAT detection relies on previously defined signatures, including IP, domain name, specific content string pattern, scripts, and others. When the monitored traffic contains one of the signatures, a corresponding alarm is triggered

for further response. Compared with others, this signature method is more reliable and convenient. Thus, it is still applied in multiple security products, ranging from intrusion detection systems (IDS) to firewall [11]. However, as the techniques used in RAT is developing, this method is seriously challenged by undetectable encrypted content because the traditional signatures are invalid to identify the malicious communications [20, 33].

In recent years, the computer security community mainly focused on machine learning techniques in encryption RAT detection [13, 14, 17, 19, 22, 34, 41, 44, 46]. Although these methods have shown significant improvements in handling the encrypted content, there are still apparent limitations among them: (1) *unstable in different environments*. Most machine learning methods try to learn the classification boundary between benign and malicious. This strategy makes the training process of models need not only malicious traffic but also benign traffic [21]. However, in different environments, the benign applications are different and keep changing day by day. In such a situation, when transferring a trained model into a different environment, the unknown applications not appeared in the training procedure can badly confuse the model. (2) *require large amounts of proper training data*. Sufficient proper data is crucial for training machine learning models. Since most training models rely on the statistical of the data, they can hardly achieve perfect performance with only limited training instances. Besides, to meet this requirement, manual preprocessing should be taken since most of the data collected from the real environment do not satisfy the input format and contains invalid records. (3) *lack of interpretability*. Most machine learning models work as black-box, which means we can only acquire a little knowledge about the results. Moreover, this mechanism can hardly help the security analyst dig out the trigger of alarms or provide knowledge about the malicious behavior.

**Our Contribution** In this paper, we study the problem of detecting encryption RAT based on network behavior analysis. Unlike the mainstream of previous research based on machine learning models, we propose a novel signature method for

RATs detection, called *Malicious network Behavior Tree (MB-Tree)*, to make up for the shortcoming of traditional signature methods in the encryption context and avoid the problems brought by machine learning methods. Motivated by the observation that RATs usually follows the fixed-code procedure to establish or release the connection, we use the *directed packet payload size (DirPiz)* of a session as primary fingerprints. As our observation, the DirPiz can be used to identify the malicious handshake, as well as handwave behaviors for encryption RAT detection. There are several advantages using DirPiz sequence as signatures: (i) effective for encrypted traffic. Since DirPiz requires no information about the traffic content, it can also adapt to the encrypted context. Moreover, in previous studies, the DirPiz sequences have already been shown effective for identifying encrypted applications and IoT devices events [26, 39]. (ii) stable in different environments. According to our observation, the DirPiz sequences of most samples keep unchanged on different machines. Thus, they can be used across different environments to acquire robust performance. (iii) convenient to extract. The DirPiz can be generated from a pcap or pcapng format file in an automated way. Compared with traditional signatures, this signature is more convenient, requiring little manual work.

However, only using DirPiz to identify encryption RAT is not precise enough. Because potential DirPiz conflicts can occur between encryption RAT and benign applications, which can increase the risk of false alarms. To tackle the challenge, we propose the *multi-level tree (MLTree)* structure as a more accurate description of the malicious behavior. Roughly, we integrate different flow-level DirPiz into host-level MLTree to improve the unique degree of malicious behaviors. Multiple malicious traces are organized in a hierarchy structure with recording the frequency of DirPiz at each level. In such a way, we can use DirPiz statistics to identify automated behavior by differentiating static packets and dynamic packets. Individually, in the interaction procedure, the distribution of DirPiz is scattered because packets transfer dynamic information like the execution results of commands. While in the automated procedure, the distribution is DirPiz is concentrated because packets transfer static information to complete specific actions.

In our design, MLTree provides several advantages. First, MLTree can capture unique malicious behavior accurately. With recording the statistics of DirPiz, the typical handshake or handwave behavior can be highlighted in MLTree to capture the malicious activities precisely. Moreover, more importantly, compared to matching a flow fingerprints DirPiz sequence, matching a host signature MLTree requires enough malicious traffic evidence. Thus the false alarms triggered by only a few coincidence DirPiz can be avoided. Second, MLTree signatures can be efficiently managed. Based on the hierarchy structure, we design a merging mechanism to integrate related signatures. Thus multiple malicious traces can be represented within a single signature to reduce the storage

cost and detection cost. Third, MLTree can be created automatically to adapt scale signatures creation. The entire signature creation procedure, including DirPiz extraction and MLTree construction, can be realized automatically with traffic pre-processing libraries. This characteristic can release security experts from tedious work of manual signature formulation.

In the detection procedure, we propose a similarity matching mechanism to replace the exact matching strategy adopted in most previous signature studies. The mechanism is designed based on MLTree structure to facilitate unique automated behavior detection. Roughly, the similarity between a testing instance and a signature consists of two parts, the handshake similarity, and the handwave similarity. Both the two parts similarity consists of a comparison of continuous edges as path score, and a comparison of diverse nodes as node score. Based on the synthesis of the four scores and the predefined threshold, it can be decided if the traffic should be regarded as malicious. Compared to the exact matching strategy, the proposed mechanism can cover deviations from the generated signatures, and adjust the alarm level of the detection by the threshold. Thus, this strategy is more flexible and appropriate for our novel signatures.

To demonstrate the effectiveness of our approach, we conduct solid experiments on two carefully designed datasets. The first dataset consists of several open source RATs traffic as the malicious part, and two public encrypted applications traffic sets as the benign part. The second dataset consists of wild trojan traffic as the malicious part and the same benign part with the first dataset. For persuasive evaluation, both datasets are divided into three parts using the stratified sampling strategy. With the strategy, we can simulate the situation that the test sets contain *unknown applications* by dividing traffic according to its applications. To acquire stable results, we also integrate the 5-fold cross-validation strategy. The experiment results show that MBTree yields a more accurate performance than machine learning state-of-the-arts on the test sets. Individually, MBTree can achieve 99% Acc and 99% F1 on the first dataset, and 98 % Acc and 89 % F1 on the second dataset. Moreover, we also inspect the malicious behaviors by tuning parameters of MBTree and inspecting generated MLTree signatures.

In summary, this paper makes the following contributions:

- We propose the MLTree structure integrating multiple DirPiz sequences as a novel signature to depict encryption RAT handshake as well as handwave behavior.
- We propose a similar based matching strategy based on MLTree to enhance the flexibility of detection.
- We show that the proposed MBTree method can adapt to the rigorous situation with limited training instances and unknown benign applications.
- We deepen the proposed MBTree by tuning parameters and analyzing the produced signatures.

## 2 Related Work

MBTree makes contributions to the problem of encryption RAT traffic detection. A central idea behind MBTree is adopting the DirPiz as signatures. Below, we discuss related works in the above areas from three perspectives.

**Machine Learning Based Encryption RAT Detection** In recent decades, machine learning methods for RAT traffic detection have been widely studied [13, 14, 17, 19, 22, 34, 41, 44, 46]. Generally, most of these methods follow such procedure that first extract features from the traffic, and then using statistical models to fit the data. Recently, [13, 17, 34, 35] use side-channel information with Random Forest (RF) for encrypted malicious traffic detection. Specifically, these side-channel features range from packet length, packet interval time to payload ratio. The experiment results have shown the effectiveness of the combination of side-channel features and machine learning models.

Besides, advanced deep learning models are also adopted in this area. Compared with traditional machine learning models, these models do not require the feature extraction procedure. The sophisticated models can automatically extract related features, and achieve end-to-end classification. For example, [22] proposes a deep learning method to detect HTTP malicious traffic on mobile networks. [46] proposes a sophisticated deep learning architecture to detect trojans with hierarchy spatiotemporal features. Generally, these traditional machine learning methods and advanced deep learning methods can achieve high performance in their experiments. However, they can hardly adapt to the situation of existing unseen applications beyond the training set. Moreover, they both lack interpretability to trace back the cause of alarms for further response.

**Signature Based RAT Detection** Compared with machine learning methods, signature methods are more robust among different environments. They aim at capturing specific malicious network fingerprints. However, there exist two limitations of traditional signature methods. First, most methods require manual work to produce high-quality signatures. This manual work is tedious for security analysts. Second, traditional signatures mainly use specific strings as signatures to identify malicious behaviors [12, 27, 29]. However, these signatures can hardly adapt to encrypted context.

In previous studies, various of them try to tackle the first problem. They mainly focus on the automatic generation of network signatures [25, 28, 32, 38]. For example, [25] propose three automatically generated signatures ranging from conjunction signatures, token-subsequence signatures to Bayes signatures for polymorphic worm detection with traffic payload. [28] uses clustered malicious traces to produce network-level signatures from HTTP fields automatically. These network-level signatures are translated in a format compatible with Snort rules and can be used for detection. However, all these studies are still blocked by the encrypted

content.

**Encrypted Traffic Identification** Encrypted network communication not only brought challenges to network defense but also to network management, like the quality of service management (QoS). As countermeasures, several studies also use machine learning methods [4, 7, 10, 18, 31, 37] and deep learning methods [2, 3, 9, 23] for encrypted traffic application classification. Recently, [9] propose a sophisticated deep learning architecture for encrypted traffic identification. Interestingly, [9] taking both reassembled payload and time related features as input. Their experiment results show a robust performance than other deep learning methods.

Apart from these researches, novel signature methods are proposed to tackle the encrypted content challenge. Instead of using specific strings as signatures, these novel methods use other perspective information to identify specific behaviors, like packet size sequence. For example, [26] propose an encrypted traffic pattern language based on *packet payload size sequence* for scalable Over-The-Top (OTT) applications identification. They show that this signature is unique to identify applications or even the application events. Similarly, [39] proposes a method based on packet length pairs to identify specific events of home IoT devices. In order to achieve the fine-grained event level traffic detection, [39] adopt the DBSCAN algorithm to search frequent conversation pairs, and then concatenate the pairs into sequences as signatures.

However, these previous studies cannot be directly used for encryption RAT detection because of listed limitations: (i) Only using a flow-level packet size sequence is not accurate enough. Since several RATs can establish different connections to evade the detection [5, 20], only flow-level fingerprints can hardly cover the whole picture of the encryption RAT behaviors. Hence, we propose an integration structure MLTree as an enhancement of DirPiz sequences for host-level detection. (ii) The exact matching strategy adopted is not flexible enough. Although the exact matching strategy can cooperate with the finite state machine to improve efficiency, it lacks the flexibility to capture similar behaviors among different environments. Hence, we propose a similar matching mechanism to facilitate the robust detection of RATs.

## 3 MBTree Overview

In this section, we provide an overview of the proposed MBTree system. As shown in Figure 1, our approach consists of two main procedures. Specifically, first, the raw traffic is formulated to MLTree, representing host-level behaviors through three steps. The preprocessing achieves traffic cleaning and session reassembling. After that, we extract the DirPiz from each session as multiple independent sequences. Next, we correlate these sequences based on common hosts and construct MLTree as the host behavior. In this procedure, malicious traffic and testing traffic follow the same steps to produce signatures and testing instances respectively. Second,

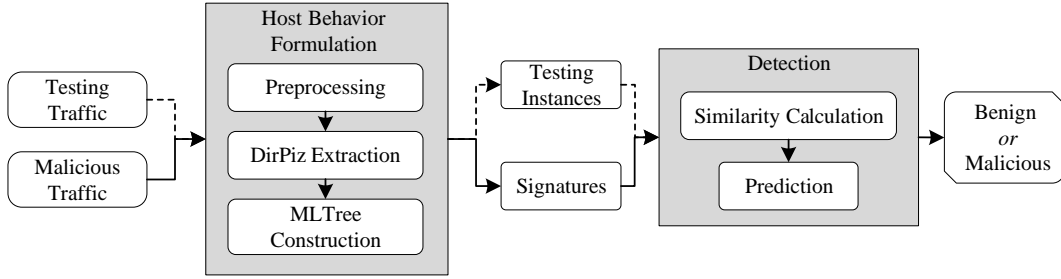


Figure 1: High-level overview of MBTree

the converted testing instances are compared to each signature to decide if they match any malicious behaviors through two steps. The first step calculates the similarity between the testing instance and each signature to produce the similarity vector. Then the second step predicts whether the instance belongs to malicious based on the similarity vector.

To show the workflow clearly, we also provide a simplified example throughout the following sections to show the key design of MBTree. The example uses a part of pure Quasar traffic as malicious traffic, and a part of mixed Quasar traffic and WhatsApp traffic as testing traffic, as shown in Figure 2.

## 4 Host Behavior Formulation

In this section, we describe the details of the formulation procedure from raw traffic to host behaviors MLTree. Section 4.1 introduces the cleaning and session reassemble strategy, Section 4.2 shows our consideration of DirPiz extraction, and Section 4.3 provides the definition of MLTree and corresponding construction process.

### 4.1 Preprocessing

The raw traffic is usually captured in pcap or pcapng format recording all communication content, including extra meta information. Since the host behavior comes from valid sessions in our consideration, we first apply traffic cleaning to discard invalid packets and session reassembling to recover these communications.

**Cleaning** Traffic cleaning aims at filtering out redundant information in raw traffic. As the requirements of cleaned traffic for signature and testing instance formulation are different, we apply different strategies for the two sets. For the training set, we apply a ‘whitelist’ strategy to only reserve the packets containing malicious IPS. Thus, only pure malicious packets are selected to produce valid signatures. For the testing set, we apply a ‘blacklist’ strategy only to discard packets that meet the following conditions: (1) repeated packets, (2) loop packets, (3) non-transmission packets. Thus, we can reserve most

of the packets in testing traffic to avoid potential malicious packets bypassing.

**Session reassembling** After cleaned, the traffic is reassembled into sessions to recover all end-to-end communication. In this procedure, we mainly based on 5-tuple to identify a transmission session. The 5-tuple includes source IP, destination IP, source port, destination port, and protocol. Besides, for TCP protocol, the flag fields representing the communication status are also used to identify unique sessions accurately.

### 4.2 DirPiz Extraction

Given a reassembled session, we extract specific DirPiz of the session as a sequence to fingerprint the automated handshake as well as handwave behavior. Specifically, a DirPiz sequence typically consists of the payload size with the direction in a connection. The direction means the packet is either request from the client to the server or response from the server to the client. As a matter of fact, multiple types of meta-information of the packet can be extracted as fingerprint, such as packet gap intervals, and packet payload hash. However, they either lack stable performance in different network environments or not adapt to variable encrypted content for the dynamic encryption key negotiation mechanism. As a result, we choose the DirPiz as the meta information for its robust performance.

Specific procedures of DirPiz sequence generation are described as following. First, we reassemble different IP packets if the fragmentation field is set. Due to the limitation of MTU or potential IP fragment attack, the communication content can be scattered in multiple IP packets. Reassembling these fragmented IP packets can restore the real payload in a communication. Second, based on these reassembled IP packets, the payload sizes are counted according to the upper-level protocols to form a sequence. This process is mainly adopted to reduce the influence of low-level protocol details, e.g., TCP handshake and SSL/TLS negotiation. For UDP protocol, the length of the transport payload is used. For TCP protocol, only the length of the transport payload in the packets is used after the connection is established. For SSL/TLS protocol,

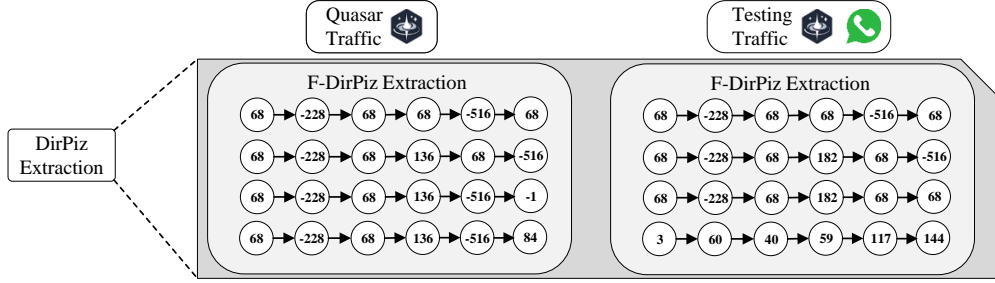


Figure 2: An example shows the simplified DirPiz sequences of each session with setting  $L$  as 6. The training set contains the malicious traffic generated from Quasar. The testing set contains the mixed traffic generated from Quasar and WhatsApp.

only the length of SSL/TLS payload in the 'Application Data' packet is used. Third, we append the direction sign to the elements of payload size sequences. The request information from a client to the server is formulated as a positive number. The response information from a server to the client is formulated as a negative number. Fourth, To focus on the automated handshake as well as the handwave process, and unify the length of sequences, we only reserve the *first  $L$  element* in the sequence as well as the *last  $L$  element* to depict the handshake and handwave behavior respectively. For sequences less than  $L$  in length, -1 is used as padding value. After that, the DirPiz sequences are generated and formatted into two parts. A real example of extracted DirPiz sequences is shown in Figure 2. The figure shows two parts of DirPiz sequences. The Quasar Traffic is used as a training set, and combined traffic, including Quasar and WhatsApp, is used as a testing set. For simplification, we set the  $L$  as six and only show the head part for both sets.

### 4.3 MLTree Construction

In this section, we construct the host behavior structure by integrating multiple diverse DirPiz sequences into MLTrees. Corresponding to use two parts of DirPiz sequences to fingerprint a session, we use two MLTrees to represent the host signature of a sample, including a head MLTree and a tail MLTree.

As a central structure of our approach, MLTree is defined as follows,

**Definition 1** *MLTree* MLTree  $T$  is a Weighted Directed Acyclic Graph (WDAG),  $T = (N, E, C_N, C_E)$ , where  $N, E, C_N, C_E$  represent the node set, edge set, node weight set, edge weight set respectively. With different to normal WDAG, MLTree is organized in hierarchy structure, every weighted node  $n_i^l$  and weighted edge  $e_i^l$  belongs to a level sub-set,  $n_i^l \in N^l, e_i^l \in E^l$ . And all these level sub-sets  $N^l, E^l, C_N^l, C_E^l$  consist of corresponding total set  $N = \{N^l\}_{l=0..L}, E = \{E^l\}_{l=0..L}, C_N = \{C_N^l\}_{l=0..L}, C_E = \{C_E^l\}_{l=0..L}$ .

From the definition, it can be seen that the MLTree consists of four elements. The node set  $N$  is used to represent unique DirPiz grouped by level. The statistical set  $C_N$  is used to record the aggregated occurrence of each unique DirPiz organized in level. The edge set  $E$  is used to represent two co-occurrence DirPiz grouped by two adjacent levels. The statistical set  $C_E$  is used to record the co-occurrences of each two adjacent DirPiz.

---

#### Algorithm 1 MLTree Construction

---

**Require:** DirPiz Sequence Set  $P$ , Max Level  $L$

**Ensure:** MLTree  $T$

- 1: Let  $T = (N, E, C_N, C_E)$
  - 2: Let  $N = \emptyset, E = \emptyset, C_N = \emptyset, C_E = \emptyset$
  - 3: **for all** level  $l \in L$  **do**
  - 4:    $N^l = \emptyset, C_N^l = \emptyset, E^l = \emptyset, C_E^l = \emptyset$
  - 5:   **for all** DirPiz sequence  $p \in P$  **do**
  - 6:      $N^l = N^l \cup \{p[l]\}, C_N^l[p[l]] + = 1$
  - 7:     **if**  $l \text{ eq } 0$  **then**
  - 8:        $e = (-1, p[l]), E^l = E^l \cup \{e\}, C_E^l[e] + = 1$
  - 9:     **else**
  - 10:        $e = (p[l-1], p[l]), E^l = E^l \cup \{e\}, C_E^l[e] + = 1$
  - 11:     **end if**
  - 12:   **end for**
  - 13:   Append  $N^l, C_N^l, E^l, C_E^l$  to  $N, C, C_N, C_E$
  - 14: **end for**
  - 15: **return**  $T$
- 

The MLTree construction process is as follows. First, the DirPiz sequences are processed level by level. In each level of processing, the nodes and edges are generated by generating unique values and corresponding statistics. Then they are appended to the MLTree. The specific schema is shown in Algorithm 1. Second, merging operations are taken to enhance the coverage as well as reduce the storage cost of repeated patterns. The specific merging algorithm is shown in Algorithm 2. However, the merging action contains *polluting risk* when integrating too much individual MLTrees into a huge

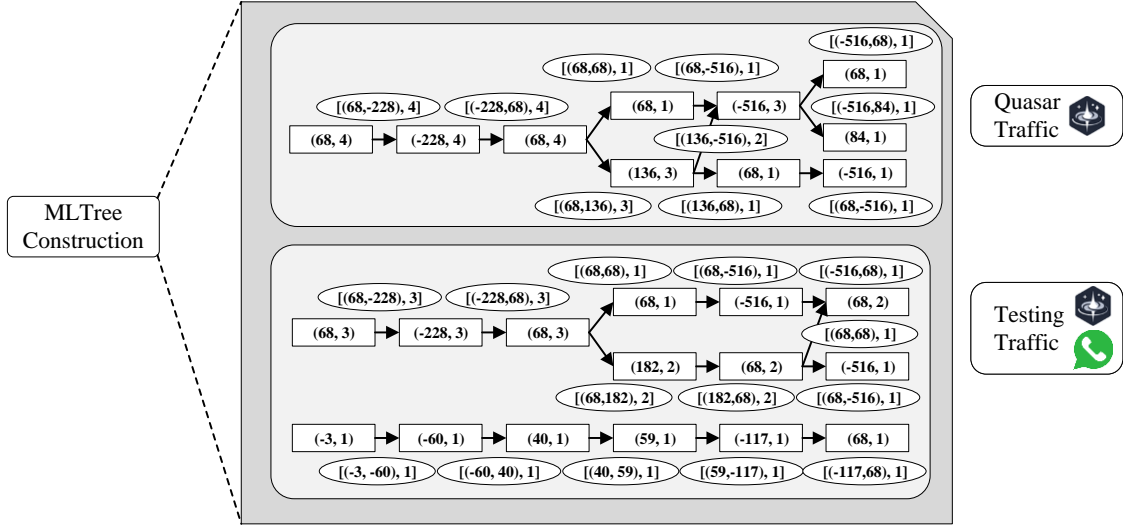


Figure 3: Corresponding generated MLTree from Figure 2. The top MLTree is generated from Quasar traffic, and the bottom MLTree is generated from testing traffic. Ovals denote the MLTree edges, and rectangles denote the MLTree nodes.

---

### Algorithm 2 MLTree Merging

---

**Require:** MLTree Set  $M$

**Ensure:** Merged MLTree  $T$

- 1: Let  $T = (N, E, C_N, C_E)$
  - 2: Let  $N = \emptyset, E = \emptyset, C_N = \emptyset, C_E = \emptyset$
  - 3: **for all** level  $l \in L$  **do**
  - 4:    $N^l = \emptyset, C_N^l = \emptyset, E^l = \emptyset, E_N^l = \emptyset$
  - 5:   **for all** MLTree  $m \in M$  **do**
  - 6:      $N^l = N^l \cup m.N^l, E^l = E^l \cup m.E^l$
  - 7:     **for all** node  $n \in N^l$ , edge  $e \in E^l$  **do**
  - 8:        $C_N^l[n] += m.C_N^l[n], C_E^l[e] += m.C_E^l[e]$
  - 9:     **end for**
  - 10:   **end for**
  - 11:   Append  $N^l, C_N^l, E^l, C_E^l$  to  $N, C, C_N, C_E$
  - 12: **end for**
  - 13: **return**  $T$
- 

MLTree. Because the coverage of the large tree will increase dramatically, resulting in high-level false alarms. To avoid this, we limit the merging operation to integrate the DirPiz sequences generated from the same sample. Thus, similar behaviors can be merged, and the scale of the tree can be limited to a proper extent. After that, the MLTree representing the host behavior of a sample is produced. As an example, the corresponding MLTrees generated from Figure 2 are shown in Figure 3. The first node (68,4) of the top MLTree represents a total 4 occurrences of DirPiz 68 in the first level of the training set. Besides, the edge[(68,-228),4] between the first node (68,4) and the second node (-228,4) of the top MLTree

represents a total 4 co-occurrence of the two DirPiz 68 and -228.

Briefly, as the host behavior, MLTree provides several advantages. First, MLTree ensures flexible merging to represent signatures efficiently. Apart from merging DirPiz, our design of MLTree can also merge different MLTrees generated from the same sample. This feature reduces the cost of storing repeated signatures; Second, the hierarchy design can represent the host behavior in an intuitive and reasonable manner. Since DirPiz sequences can be organized hierarchically to facilitate the statistics of DirPiz at different communication locations, automated handshake behavior can be quantified by differentiating between frequent DirPizs and infrequent DirPizs at each level. Because the frequent DirPiz is with a higher probability of being generated automatically. Third, MLTree can be automatically constructed. Both the MLTree construction and merging can be completed with a systematic script. In such a manner, the construction requires no interactions with security experts and prior knowledge, and the labor costs can be reduced.

## 5 Detection

Unlike traditional signature-based detection using the exact matching strategy, our detection relies on the similarity matching strategy to decide if the testing instance should be regarded as malicious. The steps of detection are as follows. First, the similarity vector of the testing instance and each signature is calculated as  $v_m = [s_0, s_1, \dots, s_n]$ . The element in the vector represents the similarity score of the testing instance and the

corresponding signature. The specific similarity score calculation method is elaborated in Section 5.1. Second, we make a prediction based on the similarity vector to decide if the testing instance contains malicious behavior. The details of this step are shown in Section 5.2.

## 5.1 Similarity Calculation

The first step towards malicious prediction is to produce the similarity vector of the testing instance. The vector is generated by comparing the testing instance with each signature in the set. Moreover, the comparison is achieved based on the MLTree similarity calculation method. In general, the similarity of two MLtrees consists of two aspects, *path similarity* and *node similarity*. The path similarity measures the similarity of continuous edges based on the statistics of edges, while the node similarity measures the similarity of nodes in corresponding hierarchies. Specifically, a similarity score  $S$  of the testing instance and a signature is formulated as

$$S = \beta[\alpha S_{fn} + (1 - \alpha)S_{fp}] + (1 - \beta)[\alpha S_{ln} + (1 - \alpha)S_{lp}] \quad (1)$$

where  $S_{fn}$  and  $S_{fp}$  represent the path similarity and the node similarity of corresponding head MLTree respectively,  $S_{ln}$  and  $S_{lp}$  represent the path similarity and the node similarity of corresponding tail MLTree respectively,  $\alpha$  represents the node ratio parameter that determines the balance of the node score and path score, and  $\beta$  represents the head ratio parameter that determines the balance of the head score and tail score.

### 5.1.1 Path Similarity

Path similarity is used to measure the common continuous paths of two MLTrees. Towards achieving this measurement, we first define *common weighted path (CWP)* as follows,

**Definition 2 Common Weighted Path** Given two MLTrees  $bt = \{N_t, E_t, C_{Nt}, C_{Et}\}$ ,  $bm = \{N_m, E_m, C_{Nm}, C_{Em}\}$ , a CWP  $P_C$  is defined as the intersection of continuous weighted edges of two MBTress. Specifically,  $I_P = \{E_t, C_{Et}\}$ , the edge set  $E_t$  is the continuous intersection of the two edge sets  $E_t$  and  $E_m$ . This means  $\forall 1 < l < L$ , if  $(n_i^l, n_j^{l+1}) \in E_t^l$ , then  $(n_i^l, n_j^{l+1}) \in (E_t \cap E_m)$ , and there exists at least one edge  $(n_p^{l-1}, n_i^l)$  that  $(n_p^{l-1}, n_i^l) \in E_t^{l-1}$ . Besides, the statistics set  $C_{Et}$  based on  $E_t$  is also the intersection of the two statistics sets according to different levels.

The CWP aims at capturing the common successive sequential information of two MLTrees. Thus, it is used as the middle-ware to measure the continuous similarity. The algorithm to generate CWP of two MLTrees is shown in Algorithm 3.

Then we provide several observations of CWP: (i) the edge statistics of CWP can reflect the similar level; (ii) the range of edge statistics at different levels in CWP is inconsistent since the edge statistics are generated independently; (iii) the

---

### Algorithm 3 CWP Generation

---

**Require:** Two MLTree  $bt = \{N_t, E_t, C_{Nt}, C_{Et}\}$ , and  $bm = \{N_m, E_m, C_{Nm}, C_{Em}\}$ , Max Level  $L$ .

**Ensure:** Common weighted path  $P_C$

```

1: Let  $P_C = \{E_C, C_{Ec}\}$ 
2: Let  $E_C = \emptyset, C_{Ec} = \emptyset$ 
3: for all level  $l \in L$  do
4:   if  $l$  is not 0 and  $E_C^{l-1}$  is  $\emptyset$  then
5:     return  $P_C$ 
6:   end if
7:   Let  $E_C^l = \emptyset, C_{Ec}^l = \emptyset, N_{imp}^l = N_t^l \cap N_m^l$ 
8:   if  $l$  is not 0 then
9:      $E_C^l = E_t^l \cap E_m^l \cap (N_{imp}^l \times N_{imp}^{l-1})$ 
10:  else
11:     $E_C^l = E_t^l \cap E_m^l$ 
12:  end if
13:  for all edge  $e \in E_C^l$  do
14:     $C_{Ec}^l = \min(C_{Et}^l[e], C_{Em}^l[e])$ 
15:  end for
16: end for
17: return  $P_C$ 

```

---

range of edge statistics at the same level in different CWP is inconsistent, since the testing instance may contain the traffic generated from a different period than signature traffic; (iv) it is of low probability to produce a long CWP between two unrelated MLTree. As a matter of fact, two unrelated MLTree may contain the same DirPiz at a level; however, they can hardly contain the same edges or even continuous edges through different levels. Thus, in general, a longer CWP indicates a higher level similarity comparing to a short CWP; and the corresponding level can be used as a weight factor of the statistics.

Next, we synthesize the observations of CWP and provide several considerations to design the formula for path similarity: (i) a higher similarity score should indicate more similar the two MLTrees are. To achieve this, we design a weighted product mechanism to ensure the monotonically increasing of the score with edge statistics and corresponding hierarchy level. (ii) the edge statistics should be normalized to be used as the base factor of the score. Specifically, we use the edge statistics of signatures at the corresponding level to normalize that of testing instance; thus, the impact of the difference among levels can be eliminated. Besides, we also introduce a time ratio to balance the period difference between the testing instance and the signature. (iii) the hierarchy level should be used as a weight factor for edge statistics. To leverage the continuous property of CWP, we assign different weights to statistics at different levels. Thus a longer CWP can correspond to higher similarity.

Based on these considerations, we tried several schemes and performed experiments on a small training set. Finally,

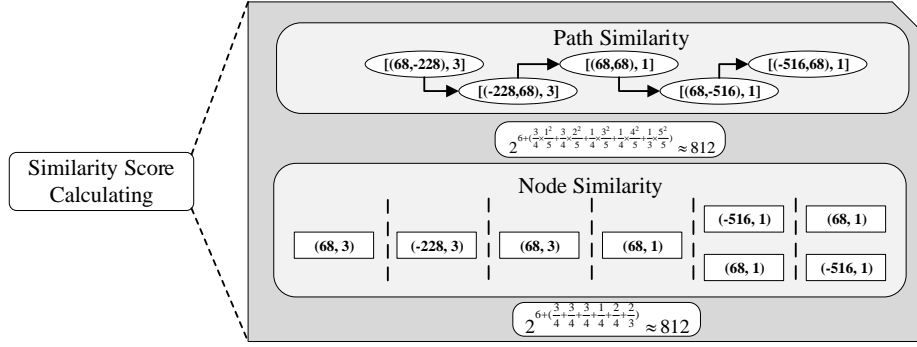


Figure 4: Similarity calculation of two MLTree in Figure 3. The top shows the CWP of the two MLTree and corresponding path similarity. The bottom shows the schematic diagram to calculate node similarity. Both  $R_l$  is set 1 in calculation.

we found the best result is achieved by the formula as follows,

$$s_p = 2^{\sum_{l=1}^{L'} [1 + \frac{F(E^l, C_E^l)}{F(E_m^l, C_{Em}^l) * R_l}] \times \frac{l^2}{L}}$$

where  $L'$  denotes the max level of CWP,  $\frac{l^2}{L}$  denotes the *level important factor*, the  $\frac{F(E^l, C_E^l)}{F(E_m^l, C_{Em}^l) * R_l}$  denotes the *normalized level path similarity factor*,  $F(a, b)$  represents *counting the total occurrence of all elements of a in set b*, and  $R_l$  denotes *the time ratio to normalize*.

### 5.1.2 Node Similarity

Node similarity is used to measure the common nodes of two MLTrees in corresponding hierarchies. As preliminary, we define the *Common Nodes* as follows.

**Definition 3 Common Nodes** The common nodes  $N_l$  are defined as the intersection nodes and their corresponding minimal occurrence at each level, formally,  $I_N = \{N_l, C_{Nl}\}, \forall l < L \rightarrow N_l^l \subseteq (N_l^l \cap N_m^l), C_{Nl}^l \subseteq (C_{Nl}^l \cap C_{Nm}^l)$ .

Totally, the node similarity is calculated based on the *common nodes*. Unlike CWP, common nodes are generated independently through different levels. Thus, the nodes are treated equally to contribute to the diverse similarity of two ML-Trees. Specifically, correspond to produce path similarity, the formula to calculate node similarity is as follows,

$$s_n = 2^{\sum_{l=1}^L (1 + \min(\frac{F(N^l, C_N^l)}{F(N_m^l, C_{Nm}^l) * R_l}, 1))}$$

where  $\min(\frac{F(N^l, C_N^l)}{F(N_m^l, C_{Nm}^l) * R_l}, 1)$  denotes the *normalized level node similarity factor*.

Unlike the path similarity measurement, the node similarity is rather simple to facilitate robust detection ability. From one

perspective, although the path similarity can accurately measure a similar path, it is not flexible enough to capture rough similar patterns. Generally, dynamically generated payloads exist in the handshake procedure, like the inspection results of the victim machine transferred by the RAT client to the server. These dynamic payloads can truncate the CWP for its random DirPiz. Hence, in such a situation, node similarity can be used as a supplementary to the path similarity to avoid false negatives. From another perspective, to avoid the global impact of explosive conflict in a single level, we limit the level node similarity factor in each level to the range of [1,2]. Thus though there exists, the influence can be limited to an acceptable level to avoid false positives.

A brief example describing the similarity calculation of two MLTrees in Figure 3 is shown in Figure 4. The calculated path similarity is around 812, and node similarity is also around 812. It should be noted that in the figure, we only showed the head MLTree comparison, and an overall similarity should also consist of the tail MLTree comparison according to Equation 1.

## 5.2 Prediction

Based on the produced similarity vector  $S_m$ , we can further predict the testing instance. First, the max value  $S_m$  of the vector  $v_m$  is specified and regarded as the malicious value of the testing instance. Then, if the  $S_m$  exceeds a predefined threshold  $\theta$ , the testing instance is regarded as containing malicious behaviors. Otherwise, the testing instance is regarded as benign. In addition, in the situation that the testing instance is regarded as malicious, the specific type of malicious behavior can also be predicted based on the index of the malicious value  $I_m$ . It is worth to mention that the specific encryption RAT type will only be decided when  $S_m$  exceeds the threshold  $\theta$ . Otherwise, it is meaningless to predict the specific RAT type since the traffic is regarded as benign.

## 6 Evaluation Framework

### 6.1 Evaluation Data

In our experiment, two malicious parts and two benign parts of traffic are used for experiments. The two malicious parts consist of the open source RATs traffic collected by ourselves, and the wild Trojan traffic selected from the Stratosphere project [36]. The two parts benign applications traffic consist of the ISCX VPN2016 [10], and the USTC-TFC2016 [42]. Each part is described below.

**Open Source Encryption RAT (OSER)** To avoid being traced, it is popular to adopt customized OSER for attack[15, 45]. Thus, the open-version RAT traffic is studied to observe their basic malicious activities. Based on popularity, stability, and maintenance on Github, 7 OSERs are selected to generate this part of the traffic. Specifically, in

Platform	Name	Transport	N1/N2
Linux	pupy	cleartext	500/500
		obfs3	300/500
		http	100/100
		SSL	100/100
		ECM	100/100
	Metasploit	RSA	500/500
		EC4+ECPV+RC4	100/100
		websocket+RSA+AES	100/100
		staged meterpreter	200/500
		stageless meterpreter	400/500
Windows	Koadic	https	150/300
	Covenant	EKE+SSL	150/300
	Stitch	AES	250/200
	QuasarRAT	TLS	100/100
	Lime-RAT	AES	100/100

Table 1: Selected open source RATs for generating malicious traffic. N1 denotes the session number in victim 1 as the training set. N2 denotes the session number in victim 2 as the testing set.

the traffic generation procedure, to evaluate whether a RAT follows the same procedure for communication in different environments, we collect the traffic of two hosts, which install different systems but are infected by the same sample. The traffic generation mechanism is shown in Figure 5. Besides, to simulate the practice usage of samples, 5 randomly chosen commands are executed on the comprised machine for each malicious session. As a result, the details of the collected traffic are shown in Table 1.

**Wild Trojan (WT)** Apart from the OSER traffic, wild trojans (from 2015 to 2018) are also selected from [36] as evaluation. Compared to OSER traffic, the WT traffic contains more number of sessions. However, since the communication between the victim and Trojan C&C cannot be controlled as detailed as OSER, it may also contain noise traffic generated by the machine automatically. Nevertheless, this part of the traffic is also a fair test to evaluate the WT detection ability of MBTree. More details of this part of the traffic are shown

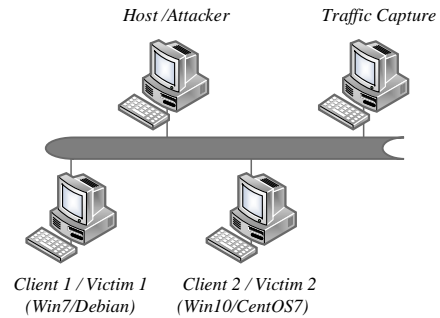


Figure 5: Traffic collection.

in Table 2.

Name	Time	Session Num	Host Num
TrickBot	2015.3-2018.4	152680	7
Emotet	2017.6	344850	9
Dridex	2017.3-2017.4	106427	13
Trickster	2017.6-2018.1	67301	3
Upatre	2015.10-2016.5	114921	2

Table 2: An overview of the WT traffic.

**ISCX VPN2016** In recent studies, the ISCX VPN2016 is widely used for encrypted traffic classification. In this paper, we also adopt this set as a part of benign traffic to evaluate the false alarm levels. Totally, the set organizes the 27G raw traffic generated from 17 typical applications in 150 pcap or pcapng files. Compared to former malicious parts, this benign application set is more large.

**USTC-TFC2016** Apart from ISCX VPN2016, we also use the benign part of USTC-TFC2016 as another part of benign traffic, because it contains different applications traffic from the ISCX VPN2016. Actually, this part of traffic consists of both benign and malicious traffic. Since the traffic contained in the malicious part of USTC-TFC2016 are relatively old (from 2011 to 2015), they are not taken as malicious part. Thus, only the benign part of the set is used for evaluation. Totally, the benign part of the USTC-TFC2016 organizes the 3.71GB traffic generated from 10 applications in 14 pcaps.

### 6.2 Data Organization

We organize the four parts of the collected traffic into two datasets for evaluation. Each dataset consists of malicious traffic and benign traffic. The OSER is used as malicious traffic in the dataset I, and the WT is used in dataset II. The benign traffic shared by two datasets is the combination of ISCX VPN2016 and USTC-TFC2016.

For persuasive evaluation, we use the 5-fold cross-evaluation strategy to acquire a stable performance. Moreover, in each fold, the dataset is divided into three parts, train,

	Dataset I			Dataset II		
	Train	Validation	Test	Train	Validation	Test
Malicious	●	●	★	▷	▷	▷
Benign	□	□	○	□	□	○

Table 3: This table shows the partitioning details in each dataset. The ● denotes the OSR traffic generated from Debian and ★ generated from CentOS; ▷ denotes the WT traffic; □ and ○ denote different applications traffic from the combination set of ISCX VPN2016 and USTC-TFC2016.

validation, and test. Basically, the three parts in a fold are divided following the ratio of 0.49:0.21:0.3. It is noteworthy that since OSER is generated from two machines, we use the traffic generated from one machine as the train and validation sets respectively, and from the other machine as the test set. Besides, the benign applications that appeared in the train set do not appear in the test set. This partitioning strategy aims at simulating the unknown applications that emerged in the test environment, which scenario is common in reality. The partition details are shown in Table 3.

### 6.3 Baselines

In correspondence to the related studies in Section 2, six baselines are covered in this paper as comparisons. The first baseline is a machine learning state-of-the-art [35] using side-channel features and CART represented as *CART*. The second baseline is another machine learning based state-of-the-art [13] using different features from [35] with random forest for Trickbot Trojan detection as *RF*. The third baseline is the extended features generated by CICFlowmeter [1] with GradientBoosting implemented by ourselves as *GBDT-CIC*. The fourth baseline is a deep learning method using a hierarchy LSTM as the architecture implemented by ourselves as *LSTM-LSTM*. The fifth baseline is a sophisticated deep learning based state-of-the-art [9] combining the content analytics and time analytics as *CETAnalytics*. Besides, we also implement the flow-level similar matching method using the cosine distance and threshold of 0.99 represented as *DirPiz-Seq* to illustrate the advantage of the host-level signatures. Moreover, we try to compare our method with ping-pong [39], which is a signature-based state-of-the-art for encrypted IOT traffic event identification. However, we find that ping-pong can hardly extract packet-level signatures of malicious traffic. Because the conversation pairs of packet-level signatures are too diverse to be clustered by the DBSCAN algorithm though we try to tune corresponding parameters.

### 6.4 Tasks & Metrics

Based on the aforementioned data, we propose the detection task for experiments. The goal of the task is to classify the traffic as generated from the general benign application or

which specific malicious application. Specifically, the malicious traffic is labeled as the specific type at the prediction. However, for benign traffic, they are all regarded equally as general benign without further classifying the specific application type.

In the experiment, four well-known metrics are adopted for comprehensive evaluation: *Accuracy (Acc)*, *F1*, *Precision (Pr)*, *Recall (Rc)* [30]. Specifically, the *macro version* of the later three metrics are used to reveal the averaged performance in predicting different classes.

## 7 Experiment

In this section, we provide a thorough evaluation of MBTree from three perspectives based on the aforementioned dataset. First, we perform the evaluation on the detection task to show the effectiveness of the proposed MBTree with comparing to several machine-learning based state-of-the-art. Second, we conduct experiments to show the influence of the hyperparameters. Further, we show the analysis of the generated signatures to reveal the network behavior differences among different samples. The hyperparameters of MBTree are set preliminary as *max level L* of 10, *path similarity ratio  $\alpha$*  of 0.3, *head signature ratio  $\beta$*  of 0.7, and *threshold  $\theta$*  as 512.

### 7.1 Malicious Detection

In this section, we focus on presenting the overall effectiveness of the proposed method MBTree. For each dataset, we first introduce the characteristics of the dataset and then show the overall superiority of our method by comparing the performance with other methods. It is noteworthy that since the concern of the paper is to detect malicious traffic rather than traffic classification, we only use the malicious traffic to build the signatures.

**Dataset I** In this dataset, the distribution of malicious and benign traffic is extremely unbalanced. Specifically, the OSER set contains exceedingly little traffic comparing to the other two public benign sets. Besides, as shown in Table 3, apart from that the benign traffic is generated from different applications in the training set and test set; the malicious traffic may also deviate between the two parts. Because they are produced from different OSs. Thus this dataset is a rigorous test for different methods.

The experiment results of this dataset are shown in Table 4. First, as a high-level performance comparison, it is apparent that the MBTree outperforms all the considered elements of comparison in both validation set and testing set in all metrics. Specifically, MBTree can achieve around 99% of Acc and F1 on the test set, which is a relatively high performance. This result demonstrate the effectiveness of MBTree design. Second, comparing the performance on validation set and test set, the signature methods including #0 and #4 performs more stable. While machine learning and deep learning methods performs

Method	Validation Set				Test Set			
	Acc(%)	F1(%)	Pr(%)	Rc(%)	Acc(%)	F1(%)	Pr(%)	Rc(%)
<b>MBTree</b>	<b>99.85±0.16</b>	<b>97.73±4.03</b>	<b>98.59±1.72</b>	98.5±2.75 †	<b>99.46±0.37</b>	<b>99.24±0.14</b>	<b>99.02±0.23</b>	<b>99.49±0.03</b>
CART [35]	99.58±0.92 †	97.67±4.32 †	98.3±2.79 †	<b>98.61±2.46</b>	63.57±28.05	65.25±10.66	73.01±9.5	67.81±9.07
RF [13]	99.36±0.94	74.31±20.19	76.15±20.25	75±19.54	56.85±20.29	46.94±2.21	59.57±0.71	46.68±3.79
GBDT-CIC	99.04±0.75	51.87±14.12	53.38±16.42	55.4±11.48	53.31±22.03	27.41±9.15	33.68±10.66	30.39±9.04
LSTM-LSTM	80.52±2.38	5.95±0.1	5.37±0.16	6.67±0	40.28±20.8	3.62±1.72	6.67±0	2.69±1.39
CETAnalytics [9]	88.24±1.47	49.39±0.01	48.38±0	53.33±0	49.44±24.24	13.36±2.51	17.9±4.21	11.26±2.15
DirPiz	80.21±9.68	83.08±1.86	81.26±2.02	92.18±2.92	84.53±3.1 †	81.18±2.15 †	81.98±2.44 †	89.41±0.82 †

Table 4: Results on Dataset I. Highlighted values: **overall best method**, second best method (†).

Method	Validation Set				Test Set			
	Acc(%)	F1(%)	Pr(%)	Rc(%)	Acc(%)	F1(%)	Pr(%)	Rc(%)
<b>MBTree</b>	<b>99.92±0.15</b>	91.42±2.77	85.76±3.97	<b>99.99±0.03</b>	<b>98.89±1.35</b>	<b>89.96±4.45</b>	<b>91.48±7.32</b>	<b>91.17±0.18</b>
CART [35]	95.67±1.1	92.41±2.04	93.07±1.68	91.86±2.33	68.19±17.99 †	44.19±17.2	47.7±13.48	49.84±19.82
RF [13]	95.92±0.48	96.07±0.86 †	<b>96.8±0.37</b>	95.45±1.27	67.62±13.01	50.04±9.89	59.23±7.02 †	55.15±11.62
GBDT-CIC	96.98±0.75	<b>96.45±1.61</b>	96.65±1.23 †	96.31±1.95 †	65.39±16.17	51.2±11.39 †	59.15±12.6	55.2±8.37
LSTM-LSTM	33.9±18.04	6.87±3.4	4.84±2.58	14.29±0	77.75±2.63	12.49±0.24	14.29±0	11.11±0.38
CETAnalytics [9]	71.78±6.09	50.24±5.05	71.53±9.05	47.16±3.05	87±4.2	38.26±12.65	38.61±11.02	51.9±15.83
DirPiz	58.2±9.39	56.33±3.7	59.73±4.77	64.53±6.47	52.84±2.15	52±2.28	58.04±5.65	60.18±3.29 †

Table 5: Results on Dataset II. Highlighted values: **overall best method**, second best method (†).

poor on validation set and even worse on the test set. This result can be mainly attributed to the limited and unbalanced training instance in OSR. In such a situation, these state-of-the-arts can hardly achieve satisfied performance. At the mean time, MBTree can properly handle the few training instances with the proposed similar matching mechanism, which can enhance the coverage of the similar behaviors without triggering false alarms.

**Dataset II** In this dataset, the malicious traffic is provided by WT. Compared to OSER, WT contains more number of malicious traffic. Besides, in this dataset, only the distribution of benign traffic may deviate between the validation set and the test set. While the malicious traffic is divided as the same into three sets with a ratio of 0.49:0.21:0.3.

The experiment results on this dataset are shown in Table 5. First, MBTree still performs stable in this dataset, which can achieve around 99% Acc and 90% F1 on both validation set and test set. It should be noted that MBTree is not achieving the high performance as in Dataset I. With analyzing the detection results, we observe that most of the misclassified instances in Dataset II consists of shorter communication sequences, which means there are only one or two valid payloads exchanged between the client and C&C. In such a case, we suspect there is no active connection established due to the silence of C&C. Second, the machine learning methods perform notably different on the validation set and test set. Although they can achieve above 95% Acc and above 90% F1 on the validation set, they can hardly handle the unknown applications and thus perform poorly in the test set. These results illustrate that the machine learning based methods are more susceptible to the change of the environment, though the malicious traffic for validation and test are produced from the same distribution. Third, it can be noticed that though

DirPiz-Seq performs well in Dataset I, it performs poorly in this dataset. The phenomenon indicates that only utilizing the flow level communication sequences as signatures is not enough. And the sophisticated design of integrating multiple flow-level sequences into host-level MLTree with corresponding similar matching mechanism performs considerably in case of sizeable malicious traffic. Fourth, although deep learning has become one of the hot research directions at present, we can see from our experiments that this technique (1) performs poorly with only limited training instances, and (2) has poor generalization ability to be adopted in practice.

As an overall assessment, MBTree outperforms all machine learning based state-of-the-art in both test sets. This demonstrates the robust detection ability in different environments, especially in the extreme case of limited and unbalanced training instances.

*Efficiency Evaluation* As a comprehensive evaluation, we also record the prediction time of each method as an efficiency comparison. The results are shown in Table 6. Compared with machine learning based approaches, MBTree cost more time for predictions than CART and RandomForest. With analyzing the workflow of the matching mechanism, we find that the main cost of our approach comes from the intersection operation in calculating the similarity score. In python, which we used for implementing MBTree, the average complexity of the intersection operation of two sets is  $O(\min(a, b))$ , where  $a, b$  refers to the length of the sets. Actually, this can be optimized by other algorithms to reduce the cost. For example, [8] have shown that the complexity of the intersection can be reduced to  $O((a + b)/\sqrt{w})$ , where  $w$  is the number of bits in a machine word. This remains as future work.

Methods	MBTree	CART	RF	GBDT-CIC	LSTM-LSTM	CETAnalytics	DirPiz-Seq
Time (s)	$10^{-3}$	$10^{-7}$	$10^{-5}$	$10^{-3}$	$10^{-3}$	$10^{-2}$	$10^{-1}$

Table 6: Prediction time of different methods for per instance.

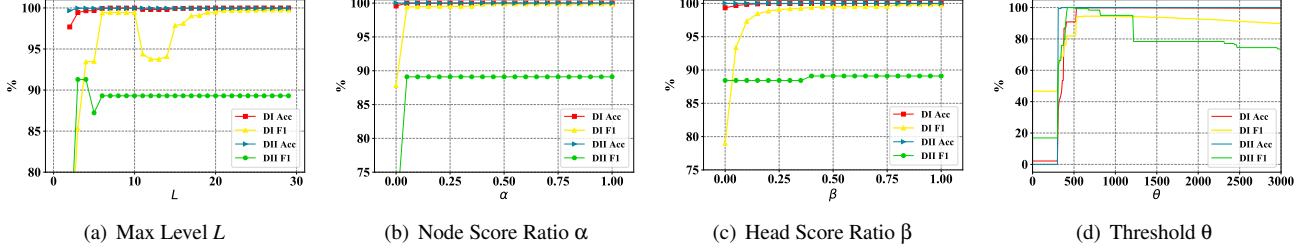


Figure 6: Different parameter tuning results. DI represents the performance on Dataset I, and DII represents the performance on Dataset II.

## 7.2 Parameter Tunning

In this section, we take experiments on the hyperparameters of MBTree to analyze their influences. Totally, there are four parameters, Max Level  $L$ , Scores Ratio  $\alpha$ ,  $\beta$  and the Threshold  $\theta$ . As adopted in previous experiments, we continue to use the default settings as start,  $L = 10$ ,  $\alpha = 0.3$ ,  $\beta = 0.7$  and threshold = 512. Results are shown in Figure 6.

**Max Level  $\theta$**  The max level  $\theta$  determines how deep should two MLTree be compared. Ideally,  $L$  is supposed to be set as exactly the length of the automated handshake procedure. However, since the handshake process implementation varies from each other, it requires experiments on  $L$  to determine the most appropriate value. Considering  $L$  and  $\theta$  are closely related, we thus choose the best performance through different  $\theta$  as the result of  $L$ . The results are shown in Figure 6(a). Based on the trend of the curves, it can be noticed that the most appropriate value of  $L$  should be chosen at the interval [3,10], which can achieve high Acc and F1 on both datasets.

**Node Score Ratio  $\alpha$**  The score ratio  $\alpha$  determines the balance of the path score and node score. Specifically,  $\alpha$  represents the ratio of the node score. The results are shown in Figure 6(b). It can be noticed that the performance rise with  $\alpha$  increasing at the initial on both datasets. This can be mainly attributed to the existence of the dynamic DirPiz in the communication sequence, which truncating the CWP. Hence, we suggest that the  $\alpha$  should be set greater than 0.1 under normal conditions to facilitate robust detection.

**Head Score Ratio  $\beta$**  The parameter  $\beta$  determines the balance of the head score and tail score. Specifically,  $\beta$  represents the ratio of the head score. The results are shown in Figure 6(c). As shown in the figure, the performances on both datasets rise with  $\beta$  increasing. Thus, it can be derived that the patterns of the handshake process are rather obvious. With the analysis of the traffic, it can be observed that the handshake process is sophisticated. The two points change information after establishing the TCP connection (e.g., the system infor-

mation). However, it is rather simple in the handwave process. The server only sends one or two packets to notify the client that the connection is closing, and then the rest work is handed over to the TCP level. Hence, we suggest that the  $\beta$  should be set greater than 0.5 without extra prior knowledge about samples.

**Threshold  $\theta$**  The parameter  $\theta$  determines the alarm level. In this experiment, we observe the performance of different  $\theta$  with setting max level  $L$  as 10. The results are shown in Figure 6(d). It can be observed from the figure that the best performance is achieved at around 512, which is slightly above the min threshold value  $0.7 \times (0.3 \times 2^{10}) + 0.3 \times (0.7 \times 2^{10}) = 430.08$ . Errors below this level are mainly caused by false negatives, which means that most of the real malicious instances are regarded as benign; and errors above this level are mainly caused by false positives, which means that most of the misclassified instances are false alarms.

## 7.3 Generated Signatures

In this section, we analyze the signature MLTrees to inspect the differences among samples by counting the number of unique values at each level. The statistics are shown in Figure 7. In this experiment, the max level  $L$  is set as 30, which is a relatively deeper value for the handshake procedure.

First, it is apparent that the unique number of most signatures is less than 50 through different levels. This appearance indicates that for most of the malicious signatures, it cost less to record the packet size as patterns. Obviously, pupy-obfs3 shows a different trend from most of the others. The DirPizs unique number of this sample is relatively high at the start of the communication. This can be attributed to that the obfs3 achieves the traffic obfuscation in the handshake procedure by changing the packet size distribution [16]. However, even though the obfuscation technology is adopted to randomize the packet size, MBTree can also effectively identify the traffic. This can be attributed to the limited range of DirPiz

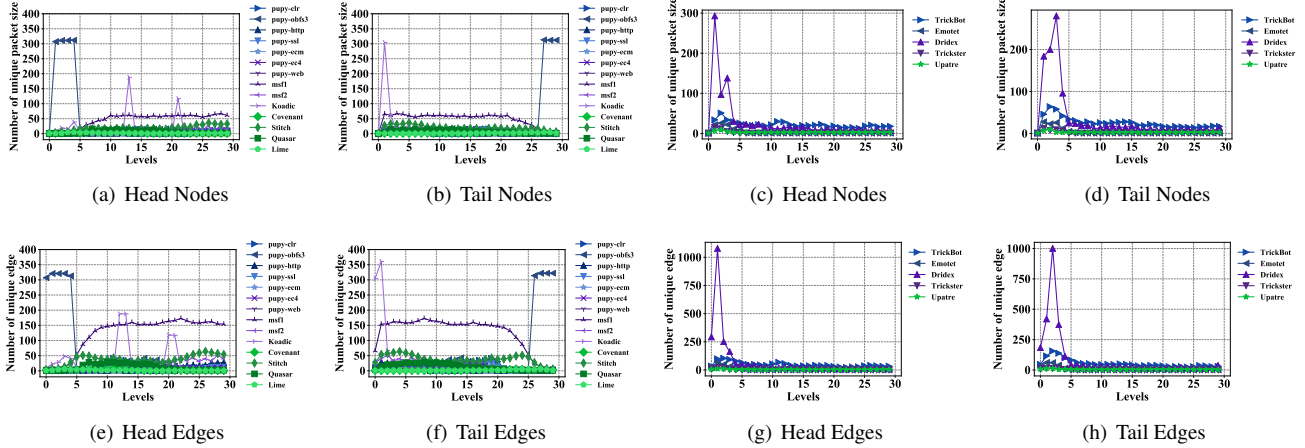


Figure 7: Number of unique values of nodes and edges organized hierarchically in the generated MLTree signatures. Figure 7(a), 7(b), 7(e), 7(f) are generated from OSER signatures. Figure 7(c), 7(d), 7(g), 7(h) are generated from WT signatures.

after randomization. Since the randomize strategy of obfs3 is applied as *using random length of bytes to pad the rest of the packet*, the length of the padded DirPiz can be only in the interval  $[raw\_content\_length, MTU]$  according to [6, 40]. Thus our designed node similarity can still cover the padded DirPiz sequences. Second, comparing the head nodes with tail nodes, it is apparent that most samples use the same packets to complete the handshake process. Thus, it can be deduced that the head patterns are slightly identical. This conclusion is also in accord with what we acquired in the experiment of  $\alpha$ . Third, rough automatic handshake length can be deduced based on the change points of the curves. For example, pupy-obfs3, msf-1, Dridex, and TrickBot accomplish the handshake process through 5 message exchanges.

## 8 Discussion

In the previous section, the experiment results illustrate that even though the content is transferred through encrypted transport, MBTree can also identify malicious communications. However, sophisticated attack strategies can still be taken by adversaries to paralysis or evade MBTree. Here we discuss the strategies that can be used against MBTree.

**Disguising Attack** A potential attack strategy for MBTree is disguising malicious traffic as benign applications. When adopting this strategy, though the malicious traces can also be identified, it will *pollute* MLTree signatures and result in a large number of false alarms to cripple the MBTree. However, in order to implement such a strategy, it requires the adversaries (i) to acquire which benign application is running; (ii) to keep on the update of the benign applications' behaviors, which is hard to achieve in practice.

**Malformed Packet** Since MBTree relies on successful payload identification, the evading techniques exploiting

the protocol stack parsing procedure can be used to evade MBTree[24, 43]. For example, transfer content through RST packets. When adopting such a technique, the payload can be incorrectly reassembled by the man-in-the-middle MBTree, and the malicious patterns cannot be identified. However, implementing this strategy also requires extra protocol stack control to deal with the malformed packets correctly. Besides, these malformed packets can be easily identified by a traditional firewall or IDS.

**Obfuscation Attack** Although our experiment proves that our MBTree can resist the obfuscation strategy to some extent, it will still lead to the invalidity of MBTree in the face of a highly targeted attack strategy. A potential obfuscation strategy is radically splitting the padded content into several packets with random packet size. In the case of such a strategy, not only MBTree will be polluted resulting in high-level false alarms, but also the sample can evade the detection of MBTree with unseen DirPiz sequences. To against this radical strategy, the entropy analysis of the DirPiz sequences can be used. Since benign applications also follow a specific procedure to complete the handshake, it is abnormal that the entropy of DirPiz sequences of a host is exceedingly high in the case of only running a few benign applications.

## 9 Conclusion

In this paper, we present the MBTree, a novel signature based approach that integrates DirPiz sequences as MLTree signatures with the similarity matching mechanism to detect encrypted RAT traffic. We evaluate MBTree against several OSERs' traffic and WTs' traffic with comprehensive benign applications' traffic as background. The results show that MBTree can detect different malicious traffic in different environments with a high-level accuracy.

## References

- [1] *cicflowmeter*. <http://netflowmeter.ca>. Retrieved November 9, 2019.
- [2] Giuseppe Aceto, Domenico Ciunzo, Antonio Montieri, and Antonio Pescapè. Mimetic: Mobile encrypted traffic classification using multimodal deep learning. *Computer Networks*, 165:106944, 2019.
- [3] Giuseppe Aceto, Domenico Ciunzo, Antonio Montieri, and Antonio Pescapè. Mobile encrypted traffic classification using deep learning: Experimental evaluation, lessons learned, and challenges. *IEEE Transactions on Network and Service Management (TNSM)*, 2019.
- [4] Riyadh Alshammari and A Nur Zincir-Heywood. Can encrypted traffic be identified without port numbers, ip addresses and payload inspection? *Computer Networks*, 55(6):1326–1350, 2011.
- [5] Manos Antonakakis, Tim April, Michael Bailey, Matt Bernhard, Elie Bursztein, Jaime Cochran, Zakir Durumeric, J Alex Halderman, Luca Invernizzi, Michalis Kallitsis, et al. Understanding the mirai botnet. In *26th USENIX Security Symposium (USENIX)*, pages 1093–1110, 2017.
- [6] Nir Bitansky and Vinod Vaikuntanathan. Indistinguishability obfuscation from functional encryption. *Journal of the ACM (JACM)*, 65(6):1–37, 2018.
- [7] Fran Casino, Kim-Kwang Raymond Choo, and Constantinos Patsakis. Hedge: efficient traffic classification of encrypted and compressed packets. *IEEE Transactions on Information Forensics and Security (TIFS)*, 14(11):2916–2926, 2019.
- [8] Bolin Ding and Arnd Christian König. Fast set intersection in memory. *Proceedings of the VLDB Endowment*, 4(4):255–266, 2011.
- [9] Cong Dong, Chen Zhang, Zhigang Lu, Baoxu Liu, and Bo Jiang. Cetanalytics: Comprehensive effective traffic information analytics for encrypted traffic classification. *Computer Networks*, page 107258, 2020.
- [10] Gerard Draper-Gil, Arash Habibi Lashkari, Mohammad Saiful Islam Mamun, and Ali A Ghorbani. Characterization of encrypted and vpn traffic using time-related. In *Proceedings of the 2nd international conference on information systems security and privacy (ICISSP)*, pages 407–414, 2016.
- [11] Alessandro D’Alconzo, Idilio Drago, Andrea Morichetta, Marco Mellia, and Pedro Casas. A survey on big data for network traffic monitoring and analysis. *IEEE Transactions on Network and Service Management (TNSM)*, 16(3):800–813, 2019.
- [12] Open Information Security Foundation. Suricata. <https://suricata-ids.org/>. Accessed February 8, 2020.
- [13] Ali Gezer, Gary Warner, Clifford Wilson, and Prakash Shrestha. A flow-based approach for trickbot banking trojan detection. *Computers & Security*, 84:179–192, 2019.
- [14] Yuanwen Huang, Swarup Bhunia, and Prabhat Mishra. Scalable test generation for trojan detection using side channel analysis. *IEEE Transactions on Information Forensics and Security (TIFS)*, 13(11):2746–2760, 2018.
- [15] Yoshihiro Ishikawa. Open source as fuel of recent apt. <https://hitcon.org/2017/pacific/0composition/pdf/Day1/R1/R1-4.12.7.pdf>. Accessed January 8, 2020.
- [16] George Kadianakis and Nick Mathewson. obfs3 (the threebfcator), jan. 2013. URL: <https://gitweb.torproject.org/pluggable-transport/obfsproxy.git/tree/doc/obfs3/obfs3-protocol-spec.txt> (cit. on p. 14).
- [17] Jiyeon Kim, Yulim Shin, Eunjung Choi, et al. An intrusion detection model based on a convolutional neural network. *Journal of Multimedia Information System*, 6(4):165–172, 2019.
- [18] Bum Jun Kwon, Virinchi Srinivas, Amol Deshpande, and Tudor Dumitraş. Catching worms, trojan horses and pups: Unsupervised detection of silent delivery campaigns. *arXiv preprint arXiv:1611.02787*, 2016.
- [19] Arash Habibi Lashkari, Andi Fitriah A Kadir, Hugo Gonzalez, Kenneth Fon Mbah, and Ali A Ghorbani. Towards a network-based framework for android malware detection and characterization. In *2017 15th Annual Conference on Privacy, Security and Trust (PST)*, pages 233–23309. IEEE, 2017.
- [20] Chaz Lever, Platon Kotzias, Davide Balzarotti, Juan Caballero, and Manos Antonakakis. A lustrum of malware network communication: Evolution and insights. In *2017 IEEE Symposium on Security and Privacy (S&P)*, pages 788–804. IEEE, 2017.
- [21] Huichen Li, Xiaojun Xu, Chang Liu, Teng Ren, Kun Wu, Xuezhi Cao, Weinan Zhang, Yong Yu, and Dawn Song. A machine learning approach to prevent malicious calls over telephony networks. In *IEEE Symposium on Security and Privacy (S&P)*, pages 53–69. IEEE, 2018.
- [22] Jia Li, Xiaochun Yun, Mao Tian, Jiang Xie, Shuhao Li, Yongzheng Zhang, and Yu Zhou. A method of http malicious traffic detection on mobile networks. In *IEEE Wireless Communications and Networking Conference (WCNC)*, pages 1–8. IEEE, 2019.
- [23] Mohammad Lotfollahi, Mahdi Jafari Siavoshani, Ramin Shirali Hossein Zade, and Mohammadsadegh Saberian. Deep packet: A novel approach for encrypted traffic classification using deep learning. *Soft Computing*, pages 1–14, 2017.
- [24] Soo-Jin Moon, Jeffrey Helt, Yifei Yuan, Yves Bieri, Sujata Banerjee, Vyas Sekar, Wenfei Wu, Mihalis Yannakakis, and Ying Zhang. Alembic: automated model inference for stateful network functions. In *USENIX Symposium on Networked Systems Design and Implementation (NSDI)*, pages 699–718, 2019.
- [25] James Newsome, Brad Karp, and Dawn Song. Polygraph: Automatically generating signatures for polymorphic worms. In *IEEE Symposium on Security and Privacy (S&P)*, pages 226–241. IEEE, 2005.
- [26] Eva Papadogiannaki, Constantinos Halevidis, Periklis Akritidis, and Lazaros Koromilas. Otter: A scalable high-resolution encrypted traffic identification engine. In *International Symposium on Research in Attacks, Intrusions, and Defenses (RAID)*, pages 315–334. Springer, 2018.

- [27] Vern Paxson. Bro: a system for detecting network intruders in real-time. *Computer Networks*, 31(23-24):2435–2463, 1999.
- [28] Roberto Perdisci, Wenke Lee, and Nick Feamster. Behavioral clustering of http-based malware and signature generation using malicious network traces. In *USENIX Symposium on Networked Systems Design and Implementation (NSDI)*, volume 10, page 14, 2010.
- [29] Martin Roesch et al. Snort: Lightweight intrusion detection for networks. In *Lisa*, volume 99, pages 229–238, 1999.
- [30] Syed Ali Raza Shah and Biju Issac. Performance comparison of intrusion detection systems and application of machine learning to snort system. *Future Generation Computer Systems*, 80:157–170, 2018.
- [31] Meng Shen, Mingwei Wei, Liehuang Zhu, and Mingzhong Wang. Classification of encrypted traffic with second-order markov chains and application attribute bigrams. *IEEE Transactions on Information Forensics and Security (TIFS)*, 12(8):1830–1843, 2017.
- [32] Kyu-Seok Shim, Sung-Ho Yoon, Su-Kang Lee, and Myung-Sup Kim. Sigbox: Automatic signature generation method for fine-grained traffic identification. *Journal of Information Science and Engineering*, 33(2):537–569, 2017.
- [33] Emily Stark, Ryan Sleevi, Rijad Muminovic, Devon O’Brien, Eran Messeri, Adrienne Porter Felt, Brendan McMillion, and Parisa Tabriz. Does certificate transparency break the web? measuring adoption and error rate. In *IEEE Symposium on Security and Privacy (S&P)*, pages 211–226. IEEE, 2019.
- [34] George Stergiopoulos, Georgia Chronopoulou, Evangelos Bitsikas, Nikolaos Tsalis, and Dimitris Gritzalis. Using side channel tcp features for real-time detection of malware connections. *Journal of Computer Security*, 27(5):507–520, 2019.
- [35] George Stergiopoulos, Alexander Talavari, Evangelos Bitsikas, and Dimitris Gritzalis. Automatic detection of various malicious traffic using side channel features on tcp packets. In *European Symposium on Research in Computer Security (ESORICS)*, pages 346–362. Springer, 2018.
- [36] Stratosphere. Stratosphere laboratory datasets. <https://www.stratosphereips.org/datasets-overview>. Retrieved November 21, 2019.
- [37] Guang-Lu Sun, Yibo Xue, Yingfei Dong, Dongsheng Wang, and Chenglong Li. An novel hybrid method for effectively classifying encrypted traffic. In *IEEE Global Telecommunications Conference (GLOBECOM)*, pages 1–5. IEEE, 2010.
- [38] Florian Tegeler, Xiaoming Fu, Giovanni Vigna, and Christopher Kruegel. Botfinder: Finding bots in network traffic without deep packet inspection. In *International Conference on emerging Networking EXperiments and Technologies (CoNEXT)*, pages 349–360, 2012.
- [39] Rahmadi Trimananda, Janus Varmarken, Athina Markopoulou, and Brian Demsky. Packet-level signatures for smart home devices. In *Network and Distributed System Security Symposium (NDSS)*, 2020.
- [40] Liang Wang, Kevin P Dyer, Aditya Akella, Thomas Ristenpart, and Thomas Shrimpton. Seeing through network-protocol obfuscation. In *ACM Conference on Computer and Communications Security (CCS)*, pages 57–69, 2015.
- [41] Shanshan Wang, Zhenxiang Chen, Qiben Yan, Bo Yang, Lizhi Peng, and Zhongtian Jia. A mobile malware detection method using behavior features in network traffic. *Journal of Network and Computer Applications*, 133:15–25, 2019.
- [42] Wei Wang, Ming Zhu, Xuewen Zeng, Xiaozhou Ye, and Yiqiang Sheng. Malware traffic classification using convolutional neural network for representation learning. In *International Conference on Information Networking (ICOIN)*, pages 712–717. IEEE, 2017.
- [43] Zhongjie Wang, Shitong Zhu, Yue Cao, Zhiyun Qian, Chengyu Song, Srikanth V Krishnamurthy, Kevin S Chan, and Tracy D Braun. Symtcp: Eluding stateful deep packet inspection with automated discrepancy discovery. In *Network and Distributed System Security Symposium (NDSS)*, 2020.
- [44] Yixin Wu, Yuqiang Sun, Cheng Huang, Peng Jia, and Luping Liu. Session-based webshell detection using machine learning in web logs. *Security and Communication Networks*, 2019, 2019.
- [45] Candid Wueest and Doherty Stephen. The increased use of powershell in attacks. *CA: Symantec Corporation World Headquarters*, pages 1–18, 2016.
- [46] Jiang Xie, Shuhao Li, Yongzheng Zhang, Xiaochun Yun, and Jia Li. A method based on hierarchical spatiotemporal features for trojan traffic detection. In *International Performance Computing and Communications Conference (IPCCC)*, pages 1–8. IEEE, 2019.